THE SUB-CRITICALITY LEVEL EFFECTS IN OPERATIONAL TRANSIENTS OF BEAM INTERRUPTION IN POWER AND STARTUP IN ACCELERATOR DRIVEN SYSTEMS

R. S. dos Santos[1,2]
[1]: Instituto de Engenharia Nuclear (CNEN/IEN)
Rua Hélio de Almeida, 75 – Cidade Universitária – Ilha do Fundão – 21945-970
Rio de Janeiro, RJ, Brazil
rsantos@ien.gov.br

[2]: Instituto Nacional de Ciência e Tecnologia de Reatores Nucleares Inovadores / CNPq

ABSTRACT

Accelerator Driven Systems (ADS) are sub-critical nuclear reactor cores driven by external spallation neutron source. These systems are currently under investigation to be used as minor actinide burners and also as transmuters of long lived fission products. The sub-criticality level plays an important rule in the control of the system. How low sub-criticality level more source dominant is the system. In this paper one analyzes two transients to analyze the feedback effect on power of the Accelerator Driven Systems, since they cover a wide range of temperature variations. These operational transients are a beam interruption in power and a startup one, when the ADS are powered up from zero power to power operation. Numerical results show that ADS can not reach the nominal operation temperatures if the systems operate next to critical ones. In a beam interruption transient systems are not affected if operated as critical ones, indicating that the initial conditions is determining for the behavior of the systems.

Keywords
ADS, Point Kinetics, Thermal Hydraulics, Feedback effects, Numerical Solutions

1. INTRODUCTION

Accelerator Driven Systems (ADS) are sub-critical nuclear reactor cores driven by external spallation neutron sources. These promising devices must be used not only as dedicated burners of transuranic elements and long-lived fission products but also as energy producers. The spallation neutrons are provided by the bombardment of a heavy metal, when impinged by proton beam, from a high energy proton accelerator [1,2].

Since a sub-critical core means that $k_{eff} < 1$, and the sub-criticality level implies the power spent to accelerate the proton beam, there is an optimum range of k_{eff} to be used in ADS.

In this paper it is analyzed the behavior of the ADS temperatures with the sub-criticality level, represented by the k_{eff} values. In this way, two transients are analyzed: beam interruption and startup transients. These transients are useful to analyze the feedback effect on power of the Accelerator Driven Systems, since they cover a wide range of temperature variations, be it a beam interruption in power or a startup one, when the ADS are powered up from zero power to power operation. For that, use was made of the SIRER-ADS code, a program based on a Point Kinetic Model. In the code, the fuel temperature, cladding and channel are solved numerically, after space and time discretization [3,4].

2. MODEL OF SIRER-ADS

The SIRER-ADS code consists of the point kinetic model, considering the external source of neutron and the thermal hydraulic of an average channel.

2.1. Thermal Hydraulic Model

As the rod is much longer than the diameter, heat flux is assumed only in radial direction. Along the coolant channel it is assumed one-dimensional. Conductivity and pressure are disregarded along the channel. The coolant flow is in a convective regime. The channel is segmented in various sections. At fuel region the heat equation is discretized assuming that temperatures are interface centered. That permits representing the hole in the centerline. The gap between fuel surface and internal surface of cladding is dealt with a resistance to the heat flux. In the fuel region the properties and temperatures are discretized as given by Fig. 1, which follows:

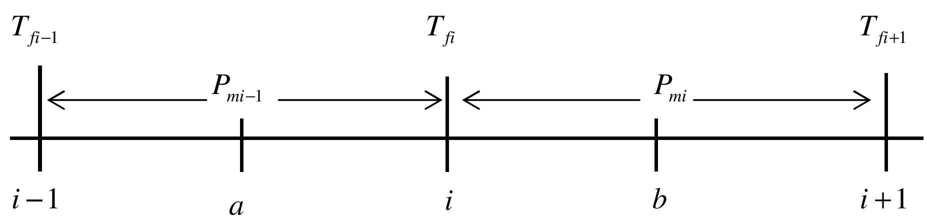

Figure 1. Temperature discretization centered at interface.

With that, a generic integration along the radius is given by:

$$\int_a^b r dr \left[\rho_m c_m \frac{\partial T_m}{\partial t} = \frac{1}{r} \frac{\partial}{\partial r} r K_m \frac{\partial T_m}{\partial r} + q_m^{'''} \right] \quad , \tag{1}$$

having in mind that m means f (fuel) or c (cladding). $P_m = P_m(r,z,t)$ can represent: ρ_m (density); c_m (specific heat); K_m (conductivity) or $q_m^{'''}$ (heat density). In the cladding T_c represents an average value in the volume and $q_m^{'''} = 0$.

For the coolant, the integration is given by:

$$\iiint dv \left(\rho_\ell c_\ell \frac{\partial T_\ell}{\partial t} = -\rho_\ell c_\ell \vec{U} . \nabla T_\ell - \nabla . \vec{q}^{\,''} \right) \quad . \tag{2}$$

Using Gauss' theorem,

$$\iiint dv \nabla . \vec{q}^{\,''} = \oiint d\vec{s} . \vec{q}^{\,''} \ , \tag{3}$$

defining the volume element $dv = A_c dz$ we have,

$$\int_{z}^{z+\Delta z} A_c dz \rho_\ell c_\ell \frac{\partial T_\ell}{\partial t} = -\int_{z}^{z+\Delta z} A_c dz \rho_\ell c_\ell U \frac{\partial T_\ell}{\partial z} - \oiint d\vec{s}.\vec{q}^{\,''} \ . \tag{4}$$

From the viewpoint of the coolant volume and using $q^{''} = h_\ell (T_{sc} - \overline{T}_\ell)$, we have:

$$\oiint d\vec{s}.\vec{q}^{\,''} = -\oiint dsq^{'''} = P_h \Delta z h_\ell \left(T_{sc} - \overline{T}_\ell\right) , \tag{5}$$

where, for triangular channels, the heated and the wetted perimeters are given by:

$$P_h = P_w = \pi R_c \, . \tag{6}$$

The discretized Eq. (1) and Eq. (2), in an axial section j, can be written in a matrix formulation given by:

$$\frac{1}{2} \underline{\underline{\mathrm{A}}} \frac{d\underline{\mathrm{X}}}{dt} = \underline{\underline{\mathrm{M}}}\underline{\mathrm{X}} + \underline{\mathrm{B}} \, , \tag{7}$$

where:

$$\underline{\underline{\mathrm{A}}} = diag(\rho_{f1}c_{f1}, \rho_{f2}c_{f2}, \rho_{f3}c_{f3}, ..., \rho_{fN-1}c_{fN-1}, \rho_{fN}c_{fN}, \rho_c c_c, \rho_\ell c_\ell) \, , \tag{8}$$

$$\underline{\mathrm{X}} = (T_{f1}, T_{f2}, T_{f3}, ..., T_{fN-1}, T_{fN}, T_c, \overline{T}_\ell) \ , \tag{9}$$

$$\underline{\mathrm{B}} = (q_{f1}^{'''}, q_{f2}^{'''}, q_{f3}^{'''}, ..., q_{fN-1}^{'''}, q_{fN}^{'''}, 0, \dot{m} c_\ell T_{\ell z} / A_c \Delta z) \ . \tag{10}$$

Redefining the matrices:

$$\underline{\underline{\mathrm{E}}} = \underline{\underline{\mathrm{A}}}^{-1} \underline{\underline{\mathrm{M}}} \ , \tag{11}$$

$$\underline{\Gamma} = \underline{\underline{\mathrm{A}}}^{-1} \underline{\mathrm{B}} \ , \tag{12}$$

we have:

$$\frac{1}{2} \frac{d\underline{\mathrm{X}}}{dt} = \underline{\underline{\mathrm{E}}}\underline{\mathrm{X}} + \underline{\Gamma} \ . \tag{13}$$

For time discretization, SIRER-ADS uses Crank-Nicholson approximation for Eq. (13), i.e.:

$$\underline{\mathrm{X}}^{n+1} = \underline{\mathrm{X}}^{n} + \frac{\Delta t}{2} \left(\frac{d\underline{\mathrm{X}}}{dt}^{n+1} + \frac{d\underline{\mathrm{X}}}{dt}^{n} \right) . \tag{14}$$

Assuming linearization on the properties during transient between time-steps like this:

$$P_m^{n+1} \cong P_m^n \ , \tag{15}$$

gives:

$$\left[\underline{\underline{I}} - \Delta t \underline{\underline{E}}^n\right]\underline{X}^{n+1} = \left[\underline{\underline{I}} + \Delta t \underline{\underline{E}}^n\right]\underline{X}^n + \Delta t\left(\Gamma^{n+1} + \Gamma^n\right) . \tag{16}$$

Redefining,

$$\underline{Y} = \left[\underline{\underline{I}} + \Delta t \underline{\underline{E}}^n\right]\underline{X}^n + \Delta t\left(\Gamma^{n+1} + \Gamma^n\right) , \tag{17}$$

the temperatures are given by:

$$\underline{X}^{n+1} = \left[\underline{\underline{I}} - \Delta t \underline{\underline{E}}^n\right]^{-1}\underline{Y} . \tag{18}$$

This inverse is easily done using the classical LU decomposition since it is a tridiagonal matrix.

2.2 Neutron Kinetic Model

According to reference [5], the point kinetic model is given by;

$$\frac{dp}{dt} = \frac{(\rho - \beta)}{\Lambda} p + \sum_{i=1}^{I} \lambda_i C_i + \frac{S}{\Lambda} , \tag{19}$$

$$\frac{dC_i}{dt} = \frac{\beta_i}{\Lambda} p - \lambda_i C_i , \; i = 1,2,3,...I , \tag{20}$$

$$\beta = \sum_{i=1}^{I} \beta_i , \tag{20}$$

$$\rho = \rho(t) = \rho(0) + \alpha_f\left[\overline{T}_f(t) - \overline{T}_f(0)\right] + \alpha_\ell\left[\overline{T}_\ell(t) - \overline{T}_\ell(0)\right] , \tag{22}$$

where $p = p(t)$ is the normalized power, $C_i = C_i(t)$ is the concentration of the i th group of delayed neutron precursor emitter, $S = S(t)$ is the external source intensity of neutron, α_f and α_ℓ are reactivity coefficients. Since the reactivity is related with k_{eff} , we have:

$$\rho(0) = \frac{k_{eff} - 1}{k_{eff}} . \tag{23}$$

In SIRER-ADS code is used Cohen's Methods for the numerical solution of point kinetic equations.

The neutronic and thermal hydraulic are coupled through:

$$q_f'''(r,z,t) = q_f'''(r,z,0)\, p(t) . \tag{24}$$

2.3 Steady-State Solution

Since Eqs. (13), (19) and (20) represent initial value problems, it is necessary to obtain the steady-state solution, which is, doing those derivatives null. In this way we have:

$$\underline{X}^0 = -\underline{\underline{E}}^{-1}\underline{\Gamma}^0 \ , \tag{25}$$

which can be done using LU decomposition.

$$C_i^0 = \frac{\beta_i}{\Lambda\lambda_i} \ , \quad i = 1,2,3,...I \ . \tag{26}$$

$$S^0 = -\rho(0) = -\rho^0 \ , \tag{27}$$

considering $p^0 = p(0) = 1$.

3. RESULTS

3.1. Steady-State Temperature Distribution

The transients to be analyzed are based on a benchmark proposed by NEA [6]. The data and description of the transient can be obtained from that reference. As one can see there, the boundary conditions are set up in such way that temperatures are fixed in 573K at the entrance and in 673K at exit channel. Thus, we need to fit the mass flow to maintain this condition. Fig. 2 exhibits the axial temperature distribution in an average channel pin in the steady-state regime.

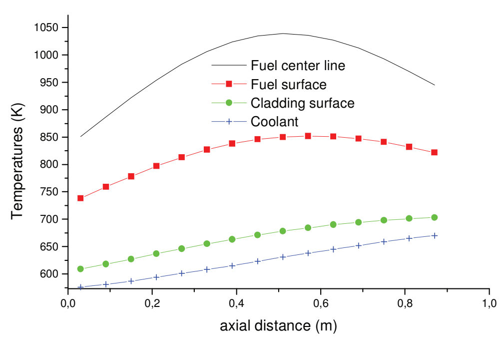

Figure 2. Steady-state temperatures.

3.2. Beam Interruption Transient

This transient simulates an interruption of the beam in an ADS, supposedly designed to operate in an continuous wave mode to generate energy, to burn actinides, or to transmute long lived fission products. The beam is interrupted for 6 second from steady state, in a transient of 10 seconds. Fig. 3 exhibits the normalized power variation. Fig. 4 and Fig. 5 show the temperature at pin center line and at channel exit, considering different sub-criticality degrees, expressed by κ_{eff} .

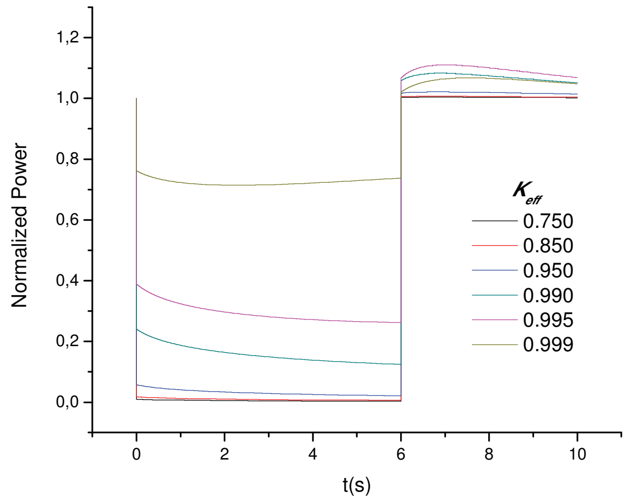

Figure 3. Normalized power versus sub-criticality level.

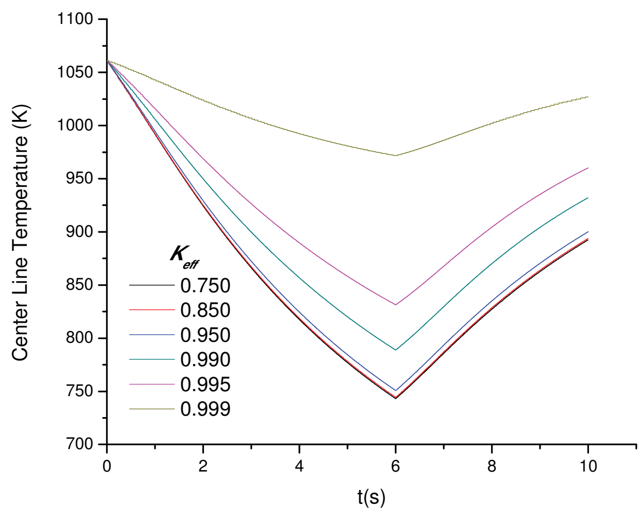

Figure 4. Pin center line temperature versus sub-criticality level.

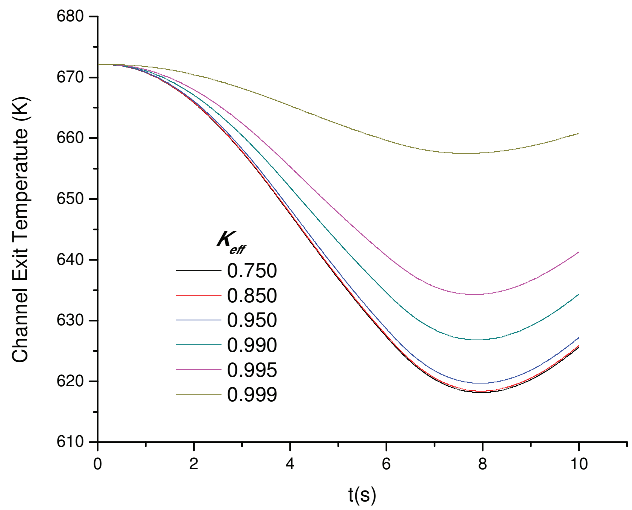

Figure 5. Channel outlet temperature versus sub-criticality level.

Fig. 6 shows the reactivity variation for different degree of sub-criticality level.

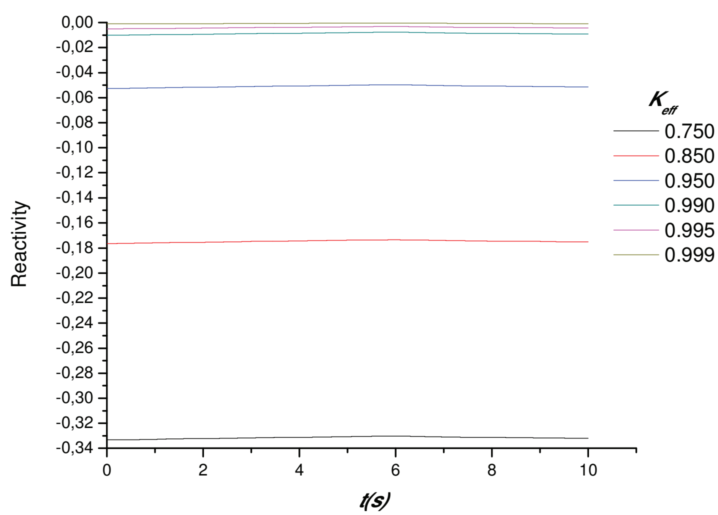

Figure 6. Reactivity versus sub-criticality level.

It is interesting to note that less sub-criticality degree implies less source dominance regime in the ADS. Fig. 7 exhibits the channel outlet temperature for complete NEA transient..

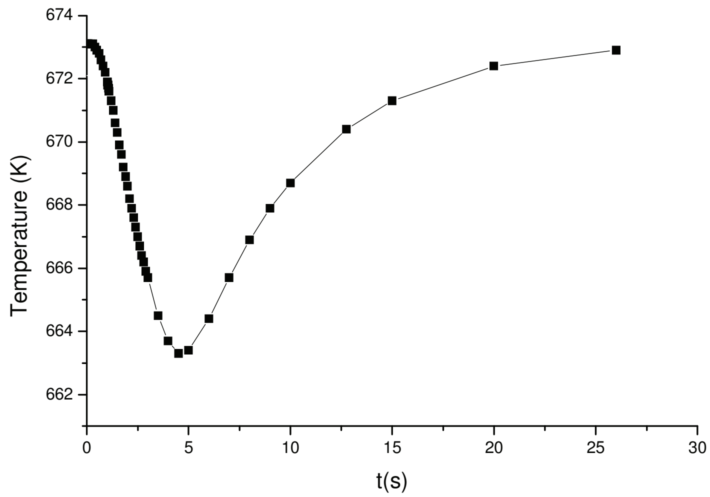

Figure 7. Channel outlet temperature in NEA during 26 seconds.

3.3. Startup Transient

This transient simulates the power up-rate of an ADS core for 20 seconds. It covers a long range of variation of the thermal properties. The temperatures vary since the hot standby condition until to the nominal power. Fig.8 shows the normalized power. Fig.9 and Fig.10 show the maximum temperature in the center line of the fuel pin and the channel outlet temperature.

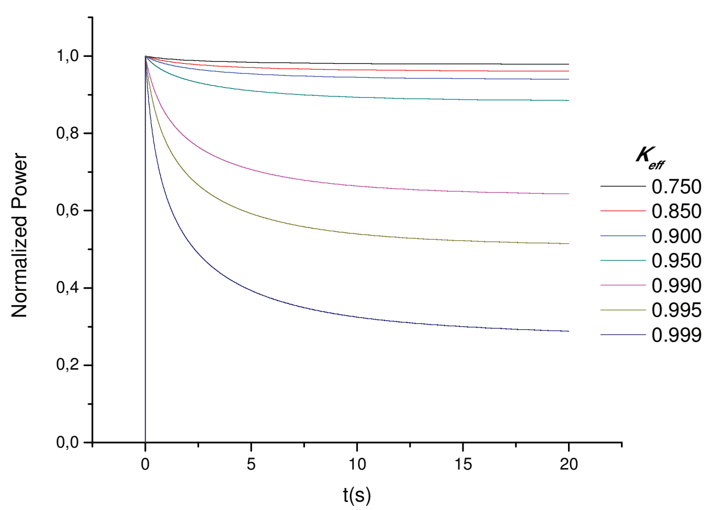

Figure 8. Normalized power versus sub-criticality level.

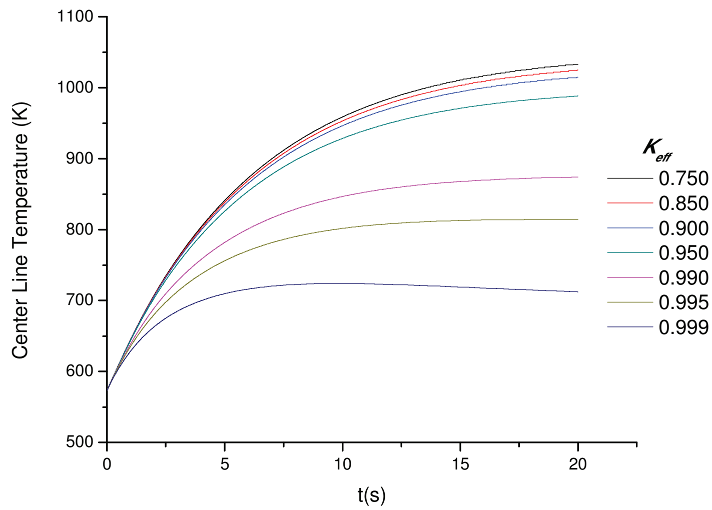

Figure 9. Pin center line temperature versus sub-criticality level.

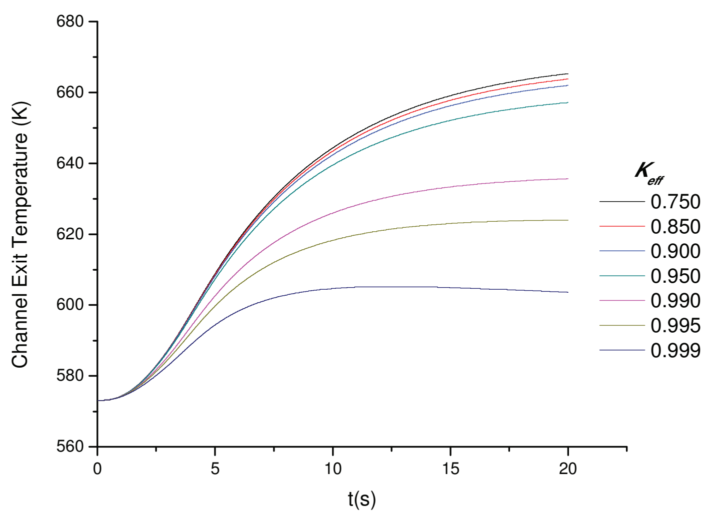

Figure 10. Channel outlet temperature versus sub-criticality level.

In this transient one observes that at low level sub-criticalities, the ADS reaches the power operation and the temperatures expected for a steady-state regime. On the other hand, sub-criticality level can impact the ADS to reach the operational level, if the sub-criticality level goes to a critical system ($k_{eff} \rightarrow 1$).

Fig. 11 shows the reactivity variation for different degree of sub-criticality level, in case of a startup transient.

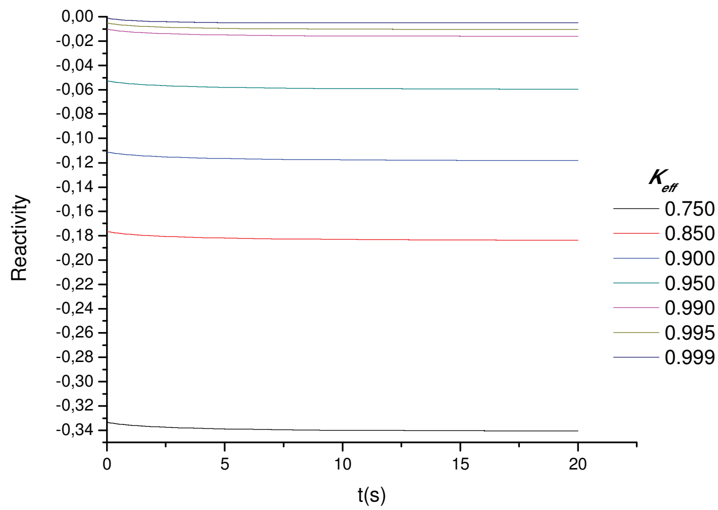

Figure 11. Reactivity versus sub-criticality level.

4. CONCLUSIONS

In this paper one analyzes the sub-criticality level effect on the ADS behavior. Numerical calculations have showed that ADS can not reach the nominal operation temperatures if the systems operate next to critical ones. While in a beam interruption transient systems are not affected if operated as critical ones, however, those systems can not reach the operational temperatures.

Although the beam interruption transient has presented plausible results, the same was not the case with the startup transient. It was clear that the initial conditions influence the behavior the simulation of the transient. This suggests a investigation on the simulation model of an ADS when analyzed with their degree of sub-criticality.

ACKNOWLEDGMENTS

I would like to thank the National Council for Scientific and Technological Development (CNPq) of Brazil, for its financial support.

REFERENCES

1. K. Tucěk, "Neutronic and Burnup Studies of Accelerator-driven System Dedicated to Nuclear Waste Transmutation," Doctoral Thesis, Royal Institute of Technology, Stockholm, 2004.
2. H. A. Abderrahim et al , " MYRRHA: A multipurpose accelerator driven system for research & development," Nuclear Instruments and Methods in Physics Research A 463, 487-994, 2001.
3. R. S., Santos and J. R., Maiorino, On the Application of SIRER_ADS in the Simulation of Transients in Accelerator Driven System (ADS), 2007 International Nuclear Atlantic Conference - INAC 2007, Santos, Brazil, 2007.

4. R.S. Santos, On Operational and Start-up Transients in an Accelerator Driven System, 2013 21st International Conference on Nuclear Engineering – ICONE 21, Chengdu, China, 2013.
5. W. M. Stacey, *Nuclear Reactor Physics,* John Wiley & Sons, New York, 2001.
6. "Benchmark on Beam Interruptions in an Accelerator-driven System: Final Report on Phase II Calculations," http://www.nea.fr/html/science/docs/2004/nsc-doc2004-7.pdf (2004).